Spin Density, T_1, T_2, T_2^* Relaxation and Bloch Equations

OVERVIEW

In this unit, we consider the four primary sources of signal variation in a standard MRI sequence. The Bloch equations that govern the motion of the magnetization as introduced in Chapter B1 must be modified to include the fact that the spins change their transverse and longitudinal orientations with time. These empirical Bloch equations (see Technical Discussion) are chosen to give the expected signal dependence based on experimental behavior.

T_1 Dependence

The solution to this more complete representation of the Bloch equations yields the following time dependence for the longitudinal component of the magnetization:

$$M_z(t) = M_z(0)e^{-t/T_1} + M_0\left(1 - e^{-t/T_1}\right) \qquad \textbf{(B3.1.1)}$$

where the term M_0 is the equilibrium magnetization and the term $M_z(0)$ represents any remnant longitudinal magnetization that still presents at time $t = 0$ from any previous manipulations of the spin system. When $M_z(0)$ is zero, the expression simplifies to

$$M_z(t) = M_0\left(1 - e^{-t/T_1}\right) \qquad \textbf{(B3.1.2)}$$

The longitudinal relaxation time (also known as the spin lattice relaxation time) T_1 represents how quickly the spins become parallel to the magnetic field. Recall that there are many spins even in a small volume and so T_1 is considered with respect to a large number of spins, but in a volume small enough to be considered much less than the spatial scales of interest (such as the voxel dimension). This small volume is referred to as an isochromat of spins. Over a very long period of time relative to T_1, the magnetization will grow to nearly its maximum value, and $M_z(t)$ will become M_0. In practice, T_1 refers to as the time it takes the signal to grow to $1 - e^{-1}$ of its maximum value (~63%). Using Equation B3.1.2, we see that in $3T_1$, the signal is at 95% of its equilibrium value. Thereafter, it only slowly increases in its value. This behavior is shown in Figure B3.1.1A, and it has very important consequences for tissue contrast in imaging sequences where multiple RF pulses are applied to completely cover k-space and the longitudinal magnetization has a limited time to regrow (see Chapter B4). For now, it is sufficient to say that if there is a 90° RF pulse applied every T_R, then the longitudinal magnetization prior to each RF pulse will be Equation B3.1.2 with t replaced by T_R, i.e.:

$$M_z(T_R) = M_0\left(1 - e^{-T_R/T_1}\right) \qquad \textbf{(B3.1.3)}$$

(The reader can see an exact derivation of the longitudinal magnetization in *UNIT B5.1*.)

Some example T_1 values for a few tissues are given in Table B3.1.1.

Contributed by Hongyu An and Weili Lin
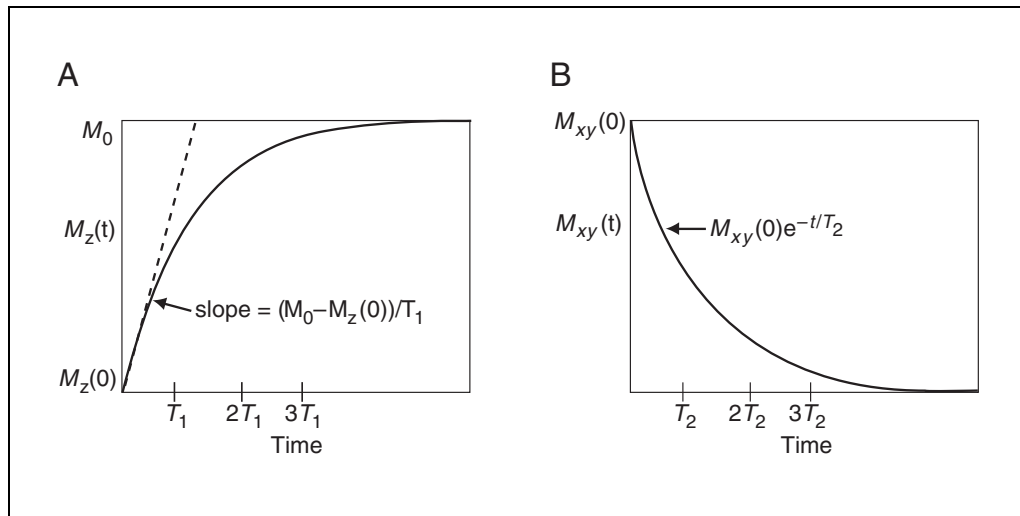
Figure B3.1.1 (**A**) The regrowth of the longitudinal component of magnetization from the initial value $M_z(0)$ to the equilibrium value M_0. (**B**) The decay of the magnitude of the transverse magnetization from an initial value.

Table B3.1.1 Representative Values of Relaxation Parameters T_1 and T_2, in msec, for Hydrogen Components of Different Human Body Tissues at B_0 = 1.5 T and 37°C (Human Body Temperature)[a]

Tissue	T_1 (msec)	T_2 (msec)
Gray matter (GM)	950	100
White matter (WM)	600	80
Muscle	900	50
Cerebrospinal fluid (CSF)	4500	2200
Fat	250	60
Blood	1200	100-200

[a]These are only approximate values. For the T_2 value of blood, the higher value pertains to arterial blood and the lower value to venous blood.

T_2 Dependence

As we have seen earlier in Chapter B2, in order to detect any signal, some transverse magnetization needs to be created. In a conventional scenario, this is done by tipping the longitudinal magnetization into the transverse plane. Assume no field inhomogeneities and the transverse magnetization immediately after an RF pulse is denoted by $M_{xy}(0)$, then:

$$M_{xy}(t) = M_{xy}(0)e^{-t/T_2} \tag{B3.1.4}$$

Basically, once a transverse magnetization exists, it quickly starts vanishing. The reason for this reduction of transverse magnetization is that local microscopic field inhomogeneities cause the spins to become irreversibly out of phase with each other, leading to signal loss. Several physical factors can account for the reduction of transverse magnetization. For example, motion of molecules whose electrons produce local fields varies as a function of time because of the molecules' motion with respect to the spin of interest. These effects are irreversible. Some example T_2 values for a few tissues are given in Table B3.1.1. Because images are usually measured about a certain time, T_E, after the RF pulse, the signal is given by

$$M_{xy}(T_E) = M_{xy}(0)e^{-T_E/T_2} \tag{B3.1.5}$$

The characteristic time T_2 is thus seen to be the time it takes for the signal to drop to $1/e$ of its original value (i.e., to 37% of its original value). This behavior is shown in Figure B3.1.1B.

Effective Spin Density

The combination of T_1 and T_2 behavior along with the spin density gives the MR signal

$$s(r) = \rho_0(r)\left(1 - e^{-T_R/T_1(r)}\right)e^{-T_E/T_2(r)} \tag{B3.1.6}$$

which gives the spatial dependence of these variables. Here $\rho_0(r)$ represents the effective spin density, where we have absorbed all other constants such as magnetic moment and its dependence on field strength and gyromagnetic ratio, etc., as well as electronic factors, including the physical spin density, all into this term.

Although the effective spin density consists of all the above mentioned constants, it is directly proportional to the number of spins per unit volume. When imaging is performed, it is considered as the number of spins per voxel. Clearly, if the voxel size is cut in half, the number of spins is also cut in half and, hence, the signal is cut in half. This speaks to why large voxels (and low resolution images) yield images with excellent signal. If we consider a high-resolution 3-D study where the voxel size is 1 mm^3, the number of excess spins parallel to the main field within this volume is greater than 10^{10}, so that even a sub-voxel on the order of 100 μm can be considered to have lots of spins in it (i.e., it serves as an isochromat).

Different tissues have different chemical compositions and different spin densities. Since most tissue is made predominantly of water, the relative spin densities of tissues for proton MRI are often given with respective to that of cerebrospinal fluid (CSF) which is itself almost 100% water. Table B3.1.2 gives some representative examples for the different tissue properties.

Table B3.1.2   Representative Value of Effective Spin Density

Tissue	$\rho_0{}^a$
Cerebrospinal fluid (CSF)	1.0
White matter (WM)	0.65
Gray matter (GM)	0.8
Fatty tissue	0.9
Blood	0.8

$^a\rho_0$ is the spin density relative to CSF.

$T_2{}^*$ Dependence

The discussion surrounding T_2 decay ignored the presence of any macroscopic field changes; however, any local variations in the background static field, regardless the sources, will also cause signal loss. This signal loss is reversible by applying a 180° pulse after the 90° pulse to refocus the spins (see *UNIT B4.1* on the spin echoes). If this refocusing

pulse is not applied, then the spins dephase, causing an extra signal reduction. The signal can be given approximately by the following expression:

$$M_{xy}(T_E) = M_{xy}(0)e^{-T_E/T_2^*} \qquad \text{(B3.1.7)}$$

where:

$$1/T_2^* = 1/T_2 + |\gamma\Delta B| \qquad \text{(B3.1.8)}$$

where ΔB is the field inhomogeneity across a voxel. To further discuss the dephasing phenomena caused by the field inhomogeneity, phase dispersion over time t can be employed. The phase is given by $\phi(r) = \gamma\Delta B(r)t$.

If spins are uniformly distributed across a voxel, then eventually the spins will have phases ranging between $-180°$ and $180°$ across the voxel. When this happens, the signal will void. Although this is not really an exponential decay, the approximation in Equation B3.1.7 above is a reasonable one for many situations and is used as an empirical formula.

These local inhomogeneities occur near the air/tissue interfaces, the mascara with iron in it, the teeth, the metal implants, etc. How rapidly the signal decays adjacent to these structures depends on the susceptibility differences with the surrounding tissue. The higher the susceptibility difference the higher ΔB and the more rapid the decay.

TECHNICAL DISCUSSION

Spin Lattice Interaction and T_1

In the presence of an external magnetic field, the spins will tend to align with it through the exchange of energy with the surrounding. Since the protons are considered to be in thermal contact with the lattice of nearby atoms, the thermal motion present in the lattice can account for any change in a given proton spin energy. The equilibrium magnetization M_0 relevant to room temperature obeys Curie's law in its dependence on the absolute temperature T and the external field:

$$M_0 = C\frac{B_0}{T} \qquad \text{(B3.1.9)}$$

where C is a constant.

In the applications to MRI, M_0 is very small compared to the maximal possible magnetization (which would be the product of the spin density and the individual spin magnetic moment). Since the proton spin energy is tiny compared with the thermal energy scale kT at room temperature, there is only a minuscule energy advantage for a spin moment to be aligned with the magnetic field. Consequently, only a small fraction of parallel spins exceed anti-parallel spins for field strengths of interest. Fortunately, Avogadro's number is so large and thus on the order of 10^{18} excess proton spins are aligned along a field strength of 0.5 T in one mole of water. Hence the magnetization M_0 is still sufficient to be measured.

Supposing the equilibrium magnetization of a body is disturbed (by the temporary application of an RF pulse) from its equilibrium value. As a result of this continued presence of the static field, the magnetization returns to its equilibrium magnetization vector, $M_0\hat{z}$.

Spin Density, T_1,
T_2, T_2^* Relaxation
and Bloch
Equations

B3.1.4

Current Protocols in Magnetic Resonance Imaging

A constant interaction growth rate from the proton interacting with the lattice implies that the rate of change of the longitudinal magnetization, $dM_z(t)/dt$, is proportional to the difference $M_0 - M_z$. The proportionality constant represents the inverse of the time scale of the growth rate. It is given by:

$$\frac{dM_z}{dt} = \frac{1}{T_1}(M_0 - M_z)$$ (B3.1.10)

The experimentally determined "spin-lattice relaxation time," T_1 has been used to characterize how fast the longitudinal magnetization can regrow to its equilibrium value.

T_1 ranges from tens to thousands of milliseconds for protons in human tissue over the B_0 field of interest (0.01 T and higher). Typical values for various tissues are shown in Table B3.1.1.

After the application of an RF pulse, the longitudinal magnetization exhibits an exponential form as a function of time, showing the evolution from the initial value, $M_z(0)$, to the equilibrium value, M_0 as a solution of Equation B3.1.10:

$$M_z(t) = M_z(0)e^{-t/T_1} + M_0\left(1 - e^{-t/T_1}\right)$$ (B3.1.11)

For an arbitrary starting point, Equation B3.1.11 can be written as:

$$M_z(t) = M_z(t_0)e^{-(t-t_0)/T_1} + M_0\left(1 - e^{-(t-t_0)/T_1}\right)$$ (B3.1.12)

When $M_z(t_0) = 0$ and $t_0 = 0$, Equation B3.1.12 can be simplified as

$$M_z(t) = M_0\left(1 - e^{-t/T_1}\right)$$ (B3.1.13)

When $t \ll T_1$, it can be further reduced as

$$M_z(t) = M_0 \cdot (t/T_1)$$ (B3.1.14)

From Equation B3.1.14, we see that there is a linear growth of the signal for a short period of time immediately after a 90° pulse. As time is prolonged, the behavior of magnetization will be governed by Equation B3.1.11 which determines how much longitudinal magnetization is available to be rotated back into the transverse plane by the next RF pulse. An illustration of the exponential regrowth for a given initial value is shown in Figure 3.1.1A.

Spin-Spin Interaction and T_2

An important mechanism for the decay of the transverse magnetization is as follows. Spins experience local fields which are combinations of the applied field and the fields of their neighbors. Since variations in the local fields lead to different local precession frequencies, each spins tends to fan out in time as shown in Figure B3.1.2, reducing the net magnetization vector. The "fanning out" is usually referred to as "dephasing." The total transverse magnetization is the vector sum of all the individual transverse components.
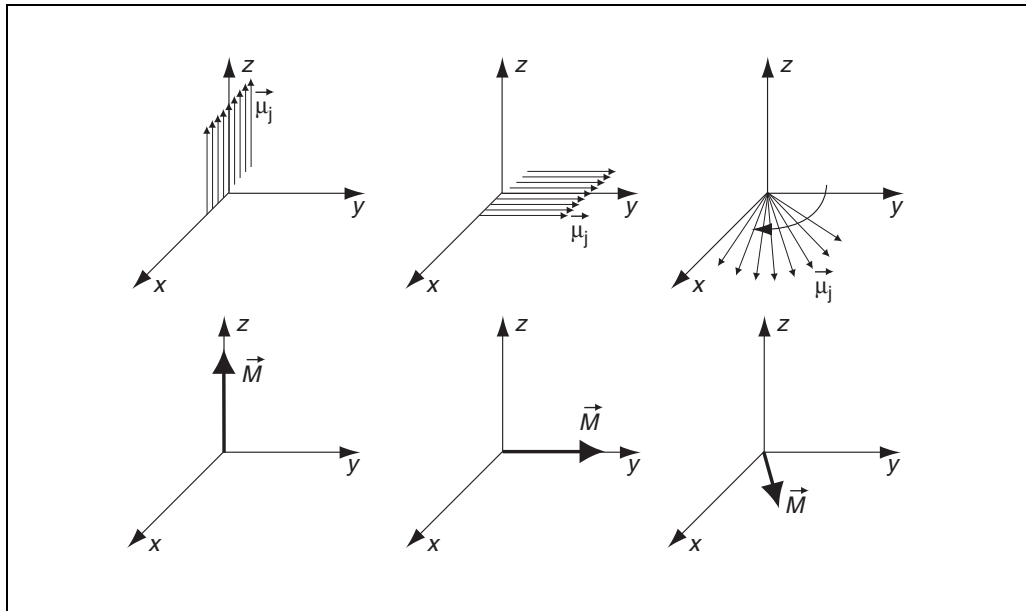
Figure B3.1.2 The upper diagrams show a 90° tip of a set of spins (isochromats) into the transverse plane such that they all lie along the *y*-axis (fixed frame) at some instant in time, as shown in the middle figure. Precession of the individual spins in the *x-y* plane immediately follows (the recovery of longitudinal magnetization is ignored since the focus is on transverse magnetization dephasing effects). The lower diagrams show the same process in terms of the net transverse magnetization which decreases in magnitude during the precession because of the fanning out of the spins.

Assuming no field inhomogeneities, the characterized time of the overall rate of reduction in transverse magnetization is denoted by the "spin-spin" relaxation time, T_2. The transverse relaxation rate R_2 is defined as $R_2 = 1/T_2$. The transverse magnetization can be described in the rotating reference frame, a reference frame which rotates clockwise around the z axis as seen from the above the origin in a fixed frame at the Larmor precession frequency, as:

$$M_{xy}(t) = M_{xy}(0)e^{-t/T_2}$$
(B3.1.15)

This equation shows that once a transverse component exists, it quickly starts vanishing. This is caused by, for example, motion of molecules whose electrons produce local fields with respect to the spin of interest. In one voxel, spins that experience different local time-dependent microscopic fields will be out of phase with each other, leading to signal loss. This signal loss is irreversible. A representive curve for the signal decay is shown in Figure B3.1.1B.

The relaxation parameter T_2 is on the order of tens of milliseconds for protons in most human tissues (see Table B3.1.1 for a variety of T_2 tissue values). It is approximately a constant over the B_0 range of interest for a given tissue. The values of T_2 are much shorter for solids (on the order of milliseconds) and much longer for liquids (on the order of seconds).

Introduction of T_2^* and T_2'

In practice, external field inhomogeneities cause time-independent field variations in a gradient echo experiment, leading to further phase dispersion across a voxel and signal loss. This effect is determined by the field distribution and the geometries of the source

**Spin Density, T_1,
T_2, T_2^* Relaxation
and Bloch
Equations**

B3.1.6

Current Protocols in Magnetic Resonance Imaging

of the field inhomogeneities. The signal behavior is complicated. But for many situations, the signal can be given approximately by a single exponential decay as:

$$M_{xy}(T_E) = M_{xy}(0)e^{-T_E/T_2^*} \tag{B3.1.16}$$

where:

$$1/T_2^* = 1/T_2 + 1/T_2'$$
$$1/T_2' = |\gamma \Delta B| \tag{B3.1.17}$$

and where ΔB is the field inhomogeneity across a voxel. We can gain insights to the understanding of the dephasing by investigating the dispersion of the phase over time. The phase is given by:

$$\phi(r) = \gamma \Delta B(r)t \tag{B3.1.18}$$

Since this local field variation is time-independent, the signal loss is reversible by applying a 180° pulse after the 90° pulse to refocus the spins (see *UNIT B4.1* on the spin echoes).

Local inhomogeneities occur near the air/tissue interfaces, mascara with iron in it, teeth, metal implants, etc. How rapidly the signal decays adjacent to these structures depends on their susceptibility differences with the surrounding tissue. The higher the susceptibility difference the larger ΔB and the more rapid the decay.

Effective Spin Density

The signal of MR imaging is commonly referred to as the amplitude (magnitude) of the spin distribution, or spin density. By name, spin density is defined as a measure of the number of spins per unit volume. However, when people talk about "spin density" in MR, what they mean is the "effective" spin density which includes other factors, such as the gyromagnetic ratio, temperature, electronic gain and main magnetic field.

The combination of T_1 and T_2 behavior along with the spin density gives the spatially dependent signal:

$$s(r) = \rho_0(r)\left(1 - e^{-T_R/T_1(r)}\right)e^{-T_E/T_2(r)} \tag{B3.1.19}$$

Here $\rho_0(r)$ represents the effective spin density.

It is well known that different body parts contain different amount of water which, in turn implies that different spin densities will be associated with different tissues. This is an important imaging/tissue parameter and provides the basic MR image contrast mechanism, in parallel to T_1 and T_2-based contrast. The relative spin densities of tissues for proton MRI are often given relative to cerebrospinal fluid (CSF) which is almost 100% water. Table B3.1.2 gives some representative examples for the different tissue properties.

Bloch Equation and Static Field Solution

An empirical vector equation, named Bloch Equation, can be utilized to characterize the magnetization in the presence of a magnetic field $\vec{B}_{ext}$ and with relaxation terms as:

$$\frac{d\vec{M}}{dt} = \gamma\vec{M} \times \vec{B}_{ext} + \frac{1}{T_1}\left(M_0 - M_z\right)\hat{z} - \frac{1}{T_2}\vec{M}_\perp \tag{B3.1.20}$$

where $\vec{M} = (M_x, M_y, M_z)$ and $\vec{M}_\perp = (M_x, M_y, 0)$.

For the constant field case, $\vec{B}_{ext} = B_0\hat{z}$, a three-component equation can be derived from Equation B3.1.20 as:

$$\frac{dM_z}{dt} = \left(M_0 - M_z\right)/T_1 \tag{B3.1.21}$$

$$\frac{dM_x}{dt} = \omega_0 M_y - M_x/T_2 \tag{B3.1.22}$$

$$\frac{dM_y}{dt} = -\omega_0 M_x - M_y/T_2 \tag{B3.1.23}$$

where $\omega_0 = \gamma B_0$.

Equations B3.1.21 to B3.1.23 can be solved as:

$$M_x(t) = e^{-t/T_2}\left(M_x(0)\cos(\omega_0 t) + M_y(0)\sin(\omega_0 t)\right) \tag{B3.1.24}$$

$$M_y(t) = e^{-t/T_2}\left(M_y(0)\cos(\omega_0 t) - M_x(0)\sin(\omega_0 t)\right) \tag{B3.1.25}$$

$$M_z(t) = M_z(0)e^{-t/T_1} + M_0\left(1 - e^{-t/T_1}\right) \tag{B3.1.26}$$

The equilibrium or steady-state solution can be found from the asymptotic limit, $t \rightarrow \infty$ of Equations B3.1.24 to B3.1.26 where all the exponentials vanish, implying the steady-state solution:

$$M_x(\infty) = M_y(\infty) = 0, \quad M_z(\infty) = M_0 \tag{B3.1.27}$$

The steady-state solution can also be found by setting all the time derivatives to zero in Equations B3.1.21 to B3.1.23 and solving them.

The general time-dependent solution for the transverse component, Equations B3.1.22 and B3.1.23, is seen to have sinusoidal terms modified by a decay factor. The sinusoidal term correspond to the precessional motion and the damping factor comes from the transverse relaxation effect. The longitudinal component relaxes from its initial value to the equilibrium value M_0; the transverse component rotates clockwise and it decreases in magnitude and eventually vanishes. Recall that the transverse decay time T_2 is in general smaller than the longitudinal decay time T_1. An example of the resulting left-handed
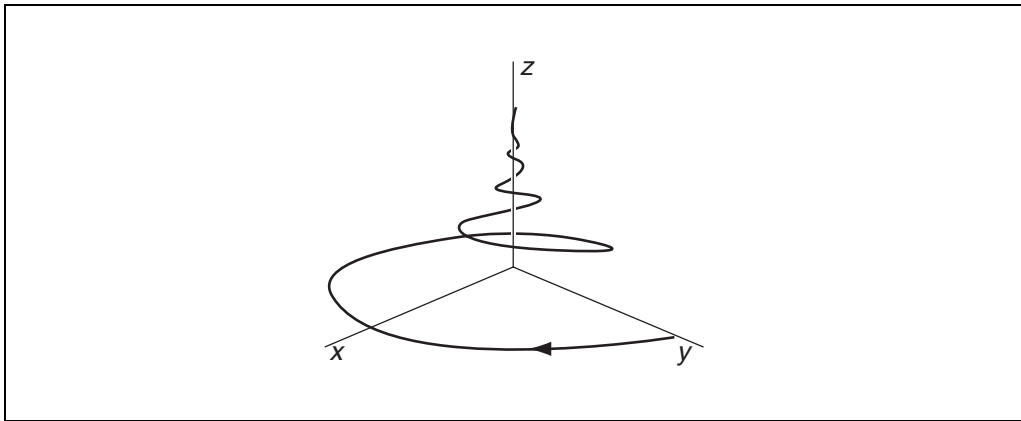
Figure B3.1.3 The trajectory of the tip of the magnetization vector showing the combined regrowth of the longitudinal magnetization and decay of the transverse components. The initial value was along the *y* axis and the reference frame is the laboratory.

trajectory for an initial magnetization lying in the transverse plane is illustrated in Figure B3.1.3.

There are several different approaches can be utilized to solve the Bloch Equations. One of them is to employ the complex representation in the *x*-*y* plane as:

$$M_+(t) = M_x + iM_y = \left| M_+(t) \right| e^{i\phi(t)} = M_\perp(t) e^{i\phi(t)} \qquad \textbf{(B3.1.28)}$$

and:

$$M_\perp(t) = e^{-t/T_2} M_\perp(0) \qquad \textbf{(B3.1.29)}$$

$$\phi(t) = -\omega_0 t + \phi(0) \qquad \textbf{(B3.1.30)}$$

where $\phi(0)$ is the initial phase and:

$$M_\perp(0)e^{i\phi(0)} = M_x(0) + iM_y(0) \qquad \textbf{(B3.1.31)}$$

By substituting Equations B3.1.29 and B3.1.30 into Equation B3.1.28, we can find that Equation B3.1.28 is identical as Equations B3.1.24 and B3.1.25.

KEY REFERENCES

Bloch, F.A. 1946. Nuclear induction. *Phys. Rev.* 70:460.

>   *This early paper discusses the basic concepts of NMR.*

Bloch, F.A., Hansen, W.W., and Packard, M. 1946a. Nuclear induction *Phys Rev.* 69:127.

>   *The fundamental NMR concepts are also provided in this paper.*

Bloch, F.A., Hansen, W.W., and Packard, M. 1946b. The nuclear induction experiment. *Phys Rev.* 70:474.

>   *More basic NMR concepts are discussed in this article.*

Basic Spin
Properties and
the Bloch
Equations

B3.1.9

Haacke, E.M., Brown, R.W., Thompson, M.R., and Venkatesan, R. 1999. Magnetic Resonance Imaging: Physical Principles and Sequence Design. John Wiley & Sons, New York.

This book covers the technical discussion here as well as other advanced materials in detail.

Purcell, E.M., Torrey, H.C., and Pound, R.V. 1946. Resonance absorption by nuclear magnetic moments in a solid. *Phys Rev*. 69:37.

This is another excellent early paper introducing the basic concepts.

Contributed by Hongyu An
Washington University
St. Louis, Missouri

Weili Lin
University of North Carolina at Chapel Hill
Chapel Hill, North Carolina

Spin Density, T_1, T_2, T_2^* Relaxation and Bloch Equations

B3.1.10